Published in final edited form as:
Ann Biomed Eng. 2013 July ; 41(7): 1411–1427. doi:10.1007/s10439-012-0695-0.

High Wall Shear Stress and Spatial Gradients in Vascular Pathology: A Review

Jennifer M. Dolan[1,3,4], **John Kolega**[1,3,4], and **Hui Meng**[1,2,3,5]

[1]Toshiba Stroke and Vascular Research Center, Clinical and Translational Research Center of the University at Buffalo, State University of New York, 875 Ellicott St., Buffalo, NY 14203, USA

[2]Department of Mechanical and Aerospace Engineering, University at Buffalo, State University of New York, Buffalo, NY 14214, USA

[3]Neuroscience Program, University at Buffalo, State University of New York, Buffalo, NY 14214, USA

[4]Department of Pathology and Anatomical Sciences, University at Buffalo, State University of New York, Buffalo, NY 14214, USA

[5]Department of Neurosurgery, University at Buffalo, State University of New York, Buffalo, NY 14214, USA

Abstract

Cardiovascular pathologies such as intracranial aneurysms (IAs) and atherosclerosis preferentially localize to bifurcations and curvatures where hemodynamics are complex. While extensive knowledge about low wall shear stress (WSS) has been generated in the past, due to its strong relevance to atherogenesis, high WSS (typically >3 Pa) has emerged as a key regulator of vascular biology and pathology as well, receiving renewed interests. As reviewed here, chronic high WSS not only stimulates adaptive outward remodeling, but also contributes to saccular IA formation (at bifurcation apices or outer curves) and atherosclerotic plaque destabilization (in stenosed vessels). Recent advances in understanding IA pathogenesis have shed new light on the role of high WSS in pathological vascular remodeling. In complex geometries, high WSS can couple with significant spatial WSS gradient (WSSG). A combination of high WSS and positive WSSG has been shown to trigger aneurysm initiation. Since endothelial cells (ECs) are sensors of WSS, we have begun to elucidate EC responses to high WSS alone and in combination with WSSG. Understanding such responses will provide insight into not only aneurysm formation, but also plaque destabilization and other vascular pathologies and potentially lead to improved strategies for disease management and novel targets for pharmacological intervention.

Keywords

Intracranial aneurysm; Aneurysm initiation; Atherosclerosis; Outward remodeling; Vulnerable plaque; Wall shear stress gradient; Endothelial cell sensing; Hemodynamics

Address correspondence to Hui Meng, Toshiba Stroke and Vascular Research Center, Clinical and Translational Research Center of the University at Buffalo, State University of New York, 875 Ellicott St., Buffalo, NY 14203, USA. huimeng@buffalo.edu.

INTRODUCTION

The ability of a blood vessel to respond to hemodynamic stimuli is mainly mediated by endothelial cells (ECs), which form the inner lining of blood vessel walls. The ECs, in direct contact with blood flow, are known sensors of the wall shear stress (WSS),[17, 18] the frictional drag exerted by blood flow acting on and parallel to the luminal surface of the endothelium. Through responses mediated by ECs, WSS regulates vessel caliber and structure,[51, 60, 62] remodeling,[29, 129] and influences the development of vascular pathologies.[71, 128]

Over four decades have been dedicated to understanding the endothelium's response to WSS, with a large focus on EC exposure to low shear stresses typically found in arterial sinuses where atherosclerotic lesions tend to develop. Such low WSS hemodynamic environments—typically associated with "disturbed flow" and characterized by flow recirculation and high oscillating shear index[14, 33, 128]—promote an atherogenic phenotype. On the other hand, baseline WSS (1.5–2.5 Pa) of straight arterial segments induces endothelial quiescence and an atheroprotective gene expression profile.[71]

Although extensive knowledge exists about EC responses in low WSS environments, until recently, little attention has been devoted to understanding EC responses to high WSS (>3 Pa). High WSS has been implicated in expansive or outward remodeling of vessels in response to a sustained increase in flow, such as in collateral arteries secondary to arterial blockage [98, 118] or in arteries feeding an arteriovenous fistula (AVF).[100, 103] Increased WSS also occurs at the entrance of a stenosed vessel[95, 96] and may contribute to atherosclerotic plaque destabilization and rupture.[102, 125] Furthermore, the apices of bifurcations and the outer sides of curved vessels are chronically exposed to higher WSS than elsewhere[2, 69]—in the cerebral vasculature, such high WSS locations are predisposed to the formation of saccular intracranial aneurysms (IAs).[39, 40, 85, 122]

In complex geometries, high WSS is often accompanied by significant spatial WSS gradient (WSSG), the spatial derivative of WSS along the flow direction with respect to the streamwise distance. Following flow impingement at a bifurcation apex, flow that splits into the daughter branches experiences rapid acceleration and then deceleration, creating regions of positive and negative spatial WSSG, respectively.[76, 79] It has been found *in vivo* that cerebral aneurysms initiate in the acceleration zone characterized by both high WSS and positive WSSG.[74, 76, 79, 123] Furthermore, computational fluid dynamic (CFD) analyses indicate that in addition to high WSS, WSSG is also significant at the throats of stenoses.[95, 96] Insight into how high WSS alone or coupled with WSSG affects EC function and subsequent vessel remodeling is important for understanding both normal vascular function and various pathological developments mediated by hemodynamics.

In this review we highlight the importance of high WSS and spatial WSSG in physiological and pathological vascular remodeling. Specifically, we focus our attention on their role in adaptive outward remodeling, IA formation, and plaque destabilization. The latter two are leading causes of morbidity and mortality in the Western World. Furthermore, we emphasize how EC responses to either high WSS alone or coupled with WSSG may mediate these pathological remodeling processes.

WSS IN THE ARTERIAL SYSTEM

WSS is the frictional drag exerted by blood flow acting on and parallel to the luminal surface of the endothelium. The magnitude of WSS in straight vessels, as estimated by Poiseuille's law, is directly proportional to the viscosity of blood and inversely proportional

to the third power of the inner radius of the vessel.[71] WSS is expressed in units of force per unit area [N/m^2 or Pascal (Pa) or dyn/cm^2, where 1 N/m^2 = 1 Pa = 10 dyn/cm^2].

Experimental measurements using different modalities have shown that over one cardiac cycle, instantaneous WSS magnitude typically ranges from 0.1 to 0.6 Pa in the venous system and from 1 to 7 Pa in straight vessels of the arterial system.[71] Since the physiological range of time-averaged WSS in straight arteries is usually between 1.5 and 2.5 Pa[51, 71] (Fig. 1a), we refer to this range as "baseline WSS." On the other hand, flow in the sinus of a bifurcation (for example the carotid artery; Fig. 1a) or inner curves of blood vessels tends to be recirculating and is often referred to as "disturbed flow." Compared to the laminar flow in straight arterial segments, it is slow and changes direction within the cardiac cycle. This produces relatively "low WSS" that is also oscillatory. Time-averaged WSS values are on the order of ±0.4 Pa in such areas.[49, 128]

A very different and less investigated flow regime can occur when flow impinges at a flow divider or the outer curve of an arterial bend to create fast, accelerating flow. This creates WSS that is higher than the baseline values mentioned above. In this review, we refer to any WSS>3 Pa as "high WSS." Near the apices of cerebral bifurcations (for example the basilar terminus; Fig. 1b), where IAs preferentially form, timed-averaged WSS can range from 11 to 34 Pa.[2, 69] High WSS also occurs at the most stenotic site of an atherosclerotic plaque (for example in the coronary artery; Fig. 1c) and has measured between 5 to over 30 Pa, depending on the degree of stenosis.[31, 63, 109, 112]

Note that, the WSS ranges denoting "low," "baseline" and "high" WSS are typical values considered for humans but do not account for individual variations. Furthermore, other species have their own baseline WSS "set-point" values for maintaining homeostasis, which may follow an allometric scaling whereby baseline WSS scales opposite to the mass of the species. [34, 124] For example, WSS in mouse aorta is almost an order of magnitude higher than that of humans.[124]

ADAPTIVE OUTWARD REMODELING: ROLE OF HIGH WSS

The function of an artery to maintain a WSS baseline appears to ensure that the metabolic needs of tissues are met while energy loss due to friction is minimized.[83] Therefore, as an adaptive response to chronically elevated high flow, an artery undergoes expansive or outward remodeling to restore WSS back to baseline levels.[52, 114, 115] Chronic flow increase usually occurs (1) in collateral arteries because of a deficiency in blood supply through a feeding artery, or (2) due to increased metabolic demand in a downstream tissue, thereby signaling a need to increase the caliber of the patent artery. This chronic flow increase results in a sustained elevation of WSS, thereby signaling outward remodeling of the vessel experiencing high WSS. Examples include an enlarging common carotid artery (CCA) when the contralateral CCA is occluded,[87] an enlarging basilar artery when both CCAs are occluded,[42] and the feeding artery of an AVF created to increase flow in the artery.[15, 99, 111, 114] In flow-induced expansion, the remodeling process is characterized by increased luminal diameter with relatively small changes in wall thickness,[64, 114] temporary and minute fragmentation of the internal elastic lamina (IEL)[42, 73, 99, 114] and proliferation of ECs and smooth muscle cells (SMCs).[73, 98, 99]

While such adaptive remodeling is normally physiological and produces healthy vessels at increased diameters, under extreme WSS increases, arterial lengthening and development of tortuosity could occur simultaneously as the lumen enlarges.[42] Severe tortuosity can predispose the artery to pathologies such as dolichoectasia, fusiform aneurysms, and atherosclerosis.[37, 42]

Endothelial Responses to Elevated WSS Mediate Adaptive Outward Remodeling

Endothelial cells mediate arterial outward remodeling stimulated by high WSS. De-endothelialized segments of the CCAs in rats fail to enlarge their lumens under increased flow.[111] WSS elevation above baseline modulates adaptive outward remodeling; when WSS returns to baseline, the vessel expansion stops, even though the flow rate remains high.[42, 53, 114]

High-WSS-stimulated outward remodeling is mediated by the endothelial signaling molecule nitric oxide, *via* the upregulation of endothelial nitric oxide synthase (eNOS). Acute vessel dilation in response to momentary flow increase is mediated by nitric oxide through smooth muscle relaxation. This does not account for the structural changes (i.e., remodeling) in flow-loaded vessels, whereby the vessel enlarges permanently, to a much greater diameter.[65, 115] However, outward remodeling subsequent to sustained flow increase also uses the nitric oxide signaling pathway.[15, 22, 36, 114–116] In studies where the second-order branches were ligated to increase flow through the mesenteric arteries, eNOS protein levels increased 2–4 days after the onset of high WSS.[22, 116] Inhibition of eNOS using long-term administration of L-NAME has partially blocked the enlargement of carotid arteries experiencing increased flow in rabbits[115] and rats.[36] Furthermore, eNOS-knockout mice fail to increase their diameter in response to high WSS even 21 days after AVF creation.[15]

High WSS Stimulates EC and SMC Proliferation During Adaptive Outward Remodeling

During high-WSS-induced outward remodeling, both ECs and SMCs proliferate in order to maintain cell coverage over the expanding wall.[73, 98, 99] AVF rabbits treated with the eNOS inhibitor L-NAME showed reduced wall tissue growth[115] thus suggesting that nitric oxide stimulates proliferation. High WSS stimulates nitric oxide-mediated EC proliferation *in vitro*.[78] Such flow-induced nitric oxide production stimulates cell proliferation probably through growth factors such as PDGF and FGF-2,[66] which increased in cultured ECs subjected to high WSS.[43, 72] In flow-loaded carotid arteries FGF-2 mRNA levels in SMCs increased post AVF creation.[101] Thus, chronic high WSS induces outward vascular remodeling through an increase in nitric oxide, which facilitates EC and SMC proliferation *via* growth factors.

High WSS Stimulates Matrix-Degrading Proteins During Adaptive Outward Remodeling

EC-mediated outward remodeling in response to high WSS requires fragmentation of the IEL.[42, 99, 114] This response is facilitated by proteolytic enzymes that degrade extracellular matrix components to increase arterial distensibility, so the vessel can expand.[15, 22, 87, 99, 114] In AVF rabbits[114] and mice[15] and rabbits experiencing increased basilar artery flow,[56] ECs and SMCs secrete matrix metalloproteinases (MMPs)-2 and -9 in response to chronic high flow.[15] Furthermore, rat[53] and rabbit[114] AVF models treated with MMP inhibitors such as doxycycline, BB-94, and RS-113,456 show diminished flow-mediated arterial enlargement and elastin degradation.[114] These observations indicate a critical role of MMPs in high-flow-induced outward remodeling. MMP activity persists until WSS is normalized.[53, 114]

Several studies using AVF models have indicated a role for nitric oxide and its downstream product peroxynitrite in regulating MMPs in flow-loaded vessels. Inhibition of nitric oxide with L-NAME decreased peroxynitrate and MMP-2 activity in ECs and the media,[114] and restricted arterial enlargement upstream of an AVF.[36, 115] In mice deficient of eNOS or the p47phox subunit of NADPH oxidase (a superoxide generator) increased flow failed to increase peroxynitrite, MMP activity, and arterial enlargement to the same degree as in wild-type animals.[15] These results indicate that both nitric oxide and superoxide, through the

generation of peroxynitrite, may be needed to activate MMPs in response to persistently increased flow.

In addition to ECs and SMCs, inflammatory cells may also mediate matrix degradation by secreting MMPs during flow-induced outward remodeling. Nuki *et al.*[87] ligated the left CCA in rats and found macrophages in the adventitia of the right CCA, which experienced flow increase. However, MMP activity was strong throughout the wall even in areas devoid of macrophages. In addition, depletion of macrophages using liposome-encapsulated clodronate reduced but did not completely block the flow-induced outward remodeling.[87] These results suggest a partial role for macrophages in outward remodeling induced by high flow.

High WSS Associates with Atherosclerotic Wall Remodeling

Atherosclerosis occurs when oxidized low-density lipoproteins, fats and other substances build up in the wall of arteries, causing the intima to thicken and plaques to form.[91] Plaque rupture can cause ischemic stroke or heart attack when an artery is obstructed by thrombosis at the rupture site or when plaque debris lodges in a downstream vessel.

While it is well known that atherogenesis occurs in disturbed flow regions with low WSS,[11, 28, 110] vessel walls with atherosclerotic plaque can experience high WSS and undergo outward or expansive remodeling as originally observed in human coronary arteries by Glagov *et al.*[32] Although outward remodeling should be beneficial by preserving luminal caliber to restore WSS to baseline levels, recent studies suggest that plaques in areas of outward remodeling are responsible for acute coronary syndromes.[97, 120] This is presumably due to thin cap rupture caused by proteolytic enzymes that facilitate the outward expansion.

It is currently unclear what factors trigger the outward remodeling in the presence of atherosclerosis. Prospective studies following plaque development in the coronary arteries over 6 months have found that areas exposed to high WSS display outward remodeling.[93, 104] Areas of high WSS were also associated with regression of fibrous and fibrofatty tissues in the plaque while developing a greater necrotic core indicating progression towards a rupture-prone phenotype.[93]

It is interesting to note that outward remodeling has also been associated with regions of low WSS.[104] In a serial study using the coronary arteries of pigs, an excessive expansive remodeling, in which the vessel and lumen are larger than non-involved areas, occurred in regions persistently experiencing low WSS.[57] This expansion is likely driven by degradation of the IEL and ECM components as low WSS promotes inflammatory cell infiltration into the wall.[16]

INTRACRANIAL ANEURYSM FORMATION: ROLE OF HIGH WSS AND WSSG

Intracranial aneurysms are pathological outpouchings of the cerebral arterial wall, characterized by loss of the IEL, media thinning with reduced number of SMCs, bulge formation, disrupted endothelium and the presence of inflammatory cells.[24, 54, 103] Although some aneurysms remain stable throughout their natural history, those that continuously experience excessive matrix degradation and mural cell death eventually rupture causing hemorrhagic stroke.[21] Saccular aneurysms, which account for approximately 90% of IAs,[127] occur most frequently at bifurcations or outer curves of arteries in the Circle of Willis, where flow impingement causes a high frictional WSS and significant flow acceleration and then deceleration, creating positive and negative WSSG, respectively.[76, 79] High WSS has long been speculated to play a role in IA pathogenesis. However, recent evidence from IA

animal studies indicates that it is the combination of high WSS and positive WSSG that precipitates IA initiation[75, 76, 79] as discussed below.

Clinical Evidence Implicates High WSS in IA Formation

Clinical and experimental observations suggest that the formation of IAs is related to high-flow hemodynamic forces. The distribution of aneurysmal lesions to the apices of bifurcations or outer curves in the Circle of Willis, where flow is complex and WSS is high, has implicated a role for hemodynamic stress as an etiological factor for IAs. It has thus been postulated that high WSS at the bifurcation contributes to IA formation.[2, 58, 103, 122] Additionally, extreme flow increases in some patients have been associated with *de novo* IA formation on the arterial pedicles that feed arteriovenous malformations[11] or in areas of the brain experiencing a compensatory flow increase as a result of carotid ligation.[45] Furthermore, several incidental human IAs imaged pre- and post-aneurysm formation [58] indicate that these aneurysms initiated at locations that were originally subjected to significantly higher WSS than the parent arteries. Collectively, these clinical observations support that high WSS is a precondition for IA natural formation.

Hemodynamic Insult Triggers IA Development in Experimental Models

The critical role of high WSS in IA formation has been supported by studies in animal models. In an early experiment, hypertension and connective tissue fragility were induced in rats, but it was only after ligation of a CCA that an aneurysm started to develop in the contralateral cerebral vasculature where blood flow was increased.[38] This suggests that despite other risk factors, flow increase is necessary for triggering IA development. It is further noted that the aneurysm most consistently examined in this model forms at a cerebral bifurcation, i.e., the junction of ophthalmic artery and anterior cerebral artery[3–7, 9, 23, 26, 46] on the contralateral side of the CCA ligation. This indicates that both elevated flow and the bifurcation hemodynamic environment are important in IA formation.

Meng and co-workers[75, 76, 123] made the first direct examination of a causal relationship between hemodynamic insult and aneurysm development *in vivo*. They induced aneurysmal remodeling in a surgically created bifurcation in which one CCA supplied both carotid territories *via* a *de novo* bifurcation consisting of naïve carotid wall[75] and correlated the remodeling with hemodynamic stresses measured in situ.[75, 76] The carotid wall, which had only been exposed to a baseline WSS before, started to experience high, impinging flow. To adapt to the new hemodynamic conditions, the wall remodeled and developed *destructive* changes that resembled early aneurysm development.[75, 76] By having a “time-zero” point, vascular change after the creation of the bifurcation could be uniquely attributable to the altered hemodynamic conditions.

This group thereafter demonstrated that hemodynamic insult can induce aneurysm formation at an existing cerebral arterial bifurcation, in the absence of other risk factors.[27, 56, 74, 79] Using CCA ligation as the only manipulation, Gao *et al.*[27] demonstrated nascent aneurysm formation at the basilar terminus in rabbits following a compensatory increase in basilar artery flow. This IA formation was dose-dependent on the basilar artery flow-rate increase, further supporting the causal relationship between flow increase and IA formation.

High WSS Combined with Positive WSSG Initiate IAs

Recognizing that IAs preferentially localize to the apices of bifurcations but not all bifurcations develop aneurysms, Meng *et al.*[75] (from our lab) sought to elucidate the specific hemodynamic conditions that predispose the apical wall to aneurysm formation. They applied a novel hemodynamic-histology co-mapping technique in their created canine carotid bifurcation by mapping hemodynamic stress distributions (from *in vivo* image-based

CFD) onto histological slices (Fig. 2a). Using this approach, they showed that the new impinging and bifurcating flow created three distinct periapical hemodynamic zones, which elicited different vascular remodeling patterns on the previously uniform carotid arterial wall[76] (Fig. 2b).

Specifically, the wall next to the bifurcation apex underwent remodeling that resembled initiation of an aneurysm, i.e., groove formation featuring disruption of the IEL, thinning of the media with loss of SMCs and loss of fibronectin.[75, 76] This destructive remodeling coincided with flow acceleration; i.e., elevated WSS and positive WSSG (Region II).[76] Meanwhile, the apex, which was exposed to impinging flow and thus low WSS (Region I), exhibited intimal hyperplasia, cell proliferation and new matrix deposition. Downstream of the acceleration region, flow decelerated toward baseline levels thereby creating negative WSSG (Region III), and no destructive changes were observed.[76] Expression of molecular markers associated with matrix degradation and aneurysm formation (MMP-2 and -9, peroxinitrite, IL-1β, and iNOS) increased in the acceleration zone relative to other hemodynamic regions.[123] These results suggest high WSS and positive WSSG provided hemodynamic conditions for aneurysmal remodeling.

Although these results were quite illuminating, they were obtained in a *created, extracranial* bifurcation. We subsequently proposed that true IA initiation is also triggered by high WSS and positive WSSG when an *existingintracranial* bifurcation is challenged by flow increase.[79] To test this hypothesis, a rabbit basilar bifurcation IA model[27, 56, 74, 79] was developed by ligating both CCAs to create an immediate compensatory flow increase through the basilar artery[42, 74] without noticeable changes in systemic blood pressure (unpublished data). Aneurysm initiating events, loss of the IEL (Fig. 3a), media thinning, and aneurysmal bulge formation were observed as early as 2 and 5 days post flow increase.[56, 79]

In order to correlate the earliest definitive aneurysmal damage with the responsible initial hemodynamic insult, Meng *et al.* imaged the rabbit basilar bifurcation immediately following CCA ligation using 3D angiography followed by CFD, and spatially mapped the initial WSS and WSSG distributions with histology of the basilar bifurcation excised at 5 days[79, 113] (Fig. 3b). IEL loss (Fig. 3a)—used as a marker of aneurysm initiation—concentrated in the acceleration zone with high WSS and high positive WSSG (Fig. 3c).[79] When each micro-segment along the basilar terminus wall was plotted on a WSS–WSSG map (denoting the local hemodynamic environment) (Fig. 3d), the IEL-damaged micro-segments dramatically segregated to high WSS and positive WSSG locations on the map while undamaged segments were associated with WSS and negative WSSG. Employing receiver operating characteristic (ROC) analysis a conservative threshold of WSS and positive WSSG (122 Pa and +530 Pa/mm), above which aneurysmal vascular damage ensues 100% of the time, was identified. [79] In addition, the degree of IA development varied among rabbits but this variation was linearly correlated with the degree of above-threshold hemodynamics that individual rabbits experienced at the basilar terminus.[79] These results suggest that a combination of high WSS and high positive WSSG above certain thresholds is responsible for aneurysm initiation.

The IA-initiating hemodynamic threshold values (Fig. 3d) found at the basilar terminus in the rabbit bilateral CCA ligation model[79] should not be considered universal. These values tend to be high since aneurysm formation in this model was induced purely by hemodynamic insult. Existence of other risk factors of IA formation (e.g., hypertension, vascular fragility) will likely lower the threshold.[77] Additionally, the threshold values for IA formation may differ by species and individuals. It is unclear whether an allometric scaling law similar to those found for baseline WSS in the aorta[34, 124] also exists for the IA

initiating WSS threshold, and whether the threshold WSSG scales as well. If such allometric scaling relationships do exist, then it might be possible to predict human WSS/WSSG values above which aneurysms may form.

Cellular and Molecular Mechanisms Underlying Flow-Induced IA Initiation

Little is known about the specific molecular mechanisms orchestrated by hemodynamics to cause IA formation. Current evidence points to impaired EC responses due to abnormal hemodynamics as the trigger for the excessive wall degeneration (including IEL loss) and cell loss, which are characteristic of aneurysmal remodeling. Light and scanning electron microscopy reveal that before aneurysm formation is evident, EC damage or loss occurs.[41, 55] Dysfunctional changes in ECs have also been noted and include decreased eNOS protein,[47, 123] depletion of tight junction proteins (occludin and ZO-1), increased vascular permeability, adhesion of leukocytes[107] and increased expression of adhesion molecules (VCAM-1 and ICAM-1) in the intima.[106]

EC dysfunction during aneurysm initiation has been attributed to the increased WSS experienced by the apex of the bifurcation. Fukuda *et al.* demonstrated that treatment of rats experiencing elevated hemodynamic stress with batroxobin, a blood viscosity reducing agent, reduced EC damage during IA formation.[26] Here, blood viscosity reduction was an effective way to reduce WSS exerted on the endothelium, thereby protecting the ECs.

Upon sensing pro-aneurysmal hemodynamic conditions, ECs must convey molecular signals to effecter cells to activate the remodeling cascades involved in IA initiation. However, EC signaling cascades have not been extensively studied under the hemodynamic conditions promoting IA formation. Recent studies in animal models by Aoki *et al.* have implicated a role for shear-responsive cyclooxygenase-2 (COX2) and prostaglandin E_2 synthase (PGES), which lead to NF-κB activation and inflammatory activity.[9] Nitric oxide has also been proposed as a signaling molecule owing to observations that eNOS protein and presumably nitric oxide bioavailability decrease during IA initiation. [47, 123] However, conflicting results using eNOS knockout mice have been reported[1, 8] and thus its role in IA formation is still ambiguous. On the other hand, superoxide, generated by the uncoupling of eNOS under oxidative conditions could also serve as a signaling molecule in aneurysm formation. Superoxide can directly activate MMPs,[89] and at high concentrations induce apoptosis.[119]

Proteolytic actions of MMPs (-2 and -9)[5] and cathepsins (B, K and S)[4] contribute to IEL loss, media thinning and luminal bulging as demonstrated by reduced IA formation in rats treated with pharmaceutical inhibitors against these proteases.[4, 5] Furthermore, proteolytic activity, in addition to oxidative cell damage, contributes to apoptosis by cleaving cell–matrix anchorage (called anoikis).[67] Cell death contributes to the characteristic media thinning of IAs.

During IA initiation upon hemodynamic triggering, MMP production and activation occur in the absence of inflammatory cell infiltration.[56] Kolega *et al.*[56] found in the rabbit IA model that IEL loss was associated with localized apoptosis and elevated MMP-2 and -9 mRNA and protein, 2 and 5 days after bilateral CCA ligation. However, inflammatory cells (macrophages and neutrophils) were almost absent and were not localized to the aneurysm initiation site at the basilar terminus.[56] Instead, a large subset of MMPs throughout the wall of the IA co-localized with alpha SM-actin, a marker of SMCs. This result suggests that at the early stage of aneurysm initiation in the rabbit model, the mural cells, rather than inflammatory infiltrates, perform inflammatory functions and produce MMPs themselves.[56]

Inflammatory cell infiltration could play an important role in IA development at later stages,[24] and/or in subjects involving etiologic factors in addition to hemodynamics alone.

In rodents receiving unilateral CCA ligation, hypertension, matrix weakening, and in some models oophorectomy to induce estrogen deficiency, [23, 46, 84] a pro-inflammatory environment was evident in the IA wall weeks or months after model creation. Pro-inflammatory changes include increased intracellular transcription factors NF-κB[7] and ets-1,[6] which leads to increases in cytokines (IL-B and MCP-1)[3, 82] and adhesion molecules (ICAM-1 and VCAM-1).[106] This leads to macrophage infiltration and its production of MMP-2 and -9.[3, 5] As a result, matrix degradation in aneurysms is widely attributed to macrophage-derived MMPs. These results indicate that, in animals loaded with multiple manipulations designed to induce IA risk factors, inflammatory cell infiltration promotes IA development at later time points.

The absence of inflammatory cells during the earliest stages of aneurysm development demonstrated in hemodynamics-only IA models (2 and 5 days as opposed to weeks or months into the process)[56] is consistent with physical intuition. High WSS in the fast, accelerating flow region next to the bifurcation apex is not conducive for monocytes attachment and infiltration. Selectin-mediated leukocyte rolling occurs at WSS near 0.4 Pa,[86] whereas the WSS at bifurcation apices in humans tends to be above 10 Pa.[2, 69] Additionally, gene expression profiling of cultured ECs indicates that WSS of 10 Pa *decreases* a number of cytokines,[21] suggesting the endothelium is not primed for inflammatory cell infiltration. However, after the aneurysmal bulge becomes more prominent, the local flow environment may change to low WSS, especially when the flow forms recirculation in the aneurysm cavity. Low WSS is more conducive to inflammatory cell infiltration, which can potently promote continued matrix degradation and cell death during aneurysm development.[24]

Hemodynamic Insult and Other Risk Factors of IA

In addition to hemodynamics, other factors, both genetic and environmental, have been associated with IA formation. These include familial history, female gender, genetic diseases (e.g., polycystic kidney disease), cigarette smoking and hypertension.[50, 90, 121] We have attempted to conceptualize the interaction between hemodynamic insult and these factors using a metaphor of a “marble in a bowl”[77] (Fig. 4).

Homeostasis is represented by a marble sitting at the bottom of the bowl, while hemodynamic insult is likened to a push on the marble (Fig. 4a). A gentle push will result in the return of the marble to the bottom and restoration of homeostasis. However, if the push is too strong (Fig. 4b), or the rim of the bowl is too low (Fig. 4c), the marble may fall out of the bowl, representing a departure from homeostasis and entry into pathogenesis (i.e., aneurysm formation).

Genetic and environmental risk factors may serve to lower the “rim” of the bowl. For example, hypertension decreases the ability of vessels to properly dilate,[88, 94] and cigarette smoking is known to induce vascular injury.[13] These factors make weaken an individual’s vasculature thus making them more susceptible to aneurysm development. While this metaphor is an over-simplification, it aids in conceptualizing the contribution of hemodynamics to IA initiation.

In short, we submit that hemodynamic insult provides the trigger for aneurysm initiation, other risk factors compromise the individual’s ability to restore homeostasis, and aneurysms develop if the hemodynamic insult (which will be most severe at bifurcations or outer curves) exceeds the system’s ability to properly adapt.

PLAQUE INSTABILITY: ROLE OF HIGH WSS AND WSSG

High WSS Contributes to Plaque Instability

Atherosclerosis is associated with morphological changes of the diseased artery. For example, the artery can undergo an expansive remodeling to preserve the lumen as discussed in “High WSS Associates with Atherosclerotic Wall Remodeling” section. However, at an unknown time point in the natural history of atherosclerotic disease the plaque can encroach into the lumen, creating vessel stenosis.[80] Plaques found in vessels experiencing lumen narrowing can be either “vulnerable,” i.e., at high risk for rupture, or stable.[125]

Plaque rupture predominately occurs in the upstream region of a stenosis.[25, 70] Lumen narrowing because of stenotic plaque results in a very unique and non-uniform WSS distribution around the plaque (Fig. 1c). Specifically, low WSS is found at the downstream shoulder of the plaque and in some cases may be oscillatory.[44] High WSS is found at the entrance of the stenosis and where the stenosis is most severe. High WSS overlying human plaque measures from 5 Pa to over 30 Pa, depending on the degree of stenosis.[31, 39, 63, 104, 112] In a study correlating plaque composition imaged using MRI with CFD simulation of WSS, Groen *et al.*[35] demonstrated that plaque ulceration occurred at a location exposed to high WSS. Since plaque rupture occurs frequently at the entrance of a stenosis where flow is increased it has been postulated that the localized high WSS contributes to plaque rupture.

Elevated WSS at the upstream segment of a plaque has also been postulated to cause mechanical rupture of the cap.[28] However, from a purely mechanics point of view, high WSS is unlikely to cause rupture since the values of WSS are markedly lower than blood pressure induced tensile stress in the cap.[68] Rupture of the plaque is thought to occur when a pressure drop induces tensile stress that exceeds the load-bearing limit of the tissue, thus leading to rupture—referred to as the fracture stress.[102] Thus high WSS produces a mechanically-negligible load on the plaque when compared to tensile stresses.

High WSS is hypothesized to modulate local biological processes that destabilize the plaque, making it more prone to rupture. In human coronary arteries, plaque thickness decreases at locations of high WSS, while thickening occurs in regions of low WSS.[93, 104] In general, cap thickness and composition of the plaque determine its fracture stress, thus reducing their integrity makes the plaque more susceptible to rupture. Regions of high WSS in human coronary artery plaques also exhibit high mechanical deformability, i.e., strain, suggesting that high WSS may modulate plaque composition.[30, 31] A review of possible mechanisms by Slager *et al.*[102] has suggested that high WSS promotes certain cellular responses such as plasmin-induced metalloproteinase activity to degrade matrix components, SMC apoptosis, and reduced matrix synthesis. Such responses under high WSS would greatly reduce cap thickness and cap stability thereby making the plaque vulnerable to rupture. High WSS at the throat of a stenosis is also implicated in platelet activation, adhesion and aggregation.[10, 48] Thus local high WSS may facilitate acute thrombus formation upon plaque rupture.

WSSG may Play a Role in Plaque Instability

Significant stenosis means that the flow velocity changes rapidly over very short distances thus creating large spatial variations in WSS. Thus both high WSS and spatial WSSG can be present in a stenosis. Schirmer and Malek [95, 96] have shown in both idealized and patient-specific stenotic geometries that WSS increased in the stenosis (>10 Pa). Furthermore, spatial WSSG increased from 80 to ~14,250 Pa/m between the upstream healthy segment of the CCA and the stenosis.[95] Although WSSG changes from positive to negative past the

throat of the stenosis, positive WSSG tends to occur in the upstream segment[95, 96] where rupture is most frequent.[25, 70]

Mounting evidence indicates that ECs have unique biological responses attributable to WSSG as discussed below. Therefore, in addition to high WSS, the presence of spatial gradients in WSS may contribute to altering pathobiology in vulnerable plaques.

ENDOTHELIAL RESPONSES TO HIGH WSS AND WSSG *IN VITRO*

High WSS Induces a Unique EC State

High WSS is receiving renewed interest due to its relevance to IA formation and atherosclerotic plaque rupture. Despite the importance of high WSS in vascular pathobiology, the specific EC response elicited by high WSS is only now beginning to be identified. Recent *in vitro* studies have revealed that high WSS induces distinct morphological and gene expression responses in ECs. As shown in Fig. 5a,[21] under high WSS, ECs elongate but do not orient to the flow direction with the same time course as cells exposed to baseline WSS.[20, 21, 78, 92] By 24 h cells under high WSS orient perpendicular to the flow[21, 78] and by 48 h they align parallel to the flow (Fig. 5a).[78]

Microarray profiling of ECs in the system shown in Fig. 5a[21] has revealed that high WSS induces a different gene expression pattern as compared to baseline WSS. High WSS upregulated genes for fibronolysis, proliferation, and matrix remodeling, downregulated pro-inflammatory cytokines[21] and increased the expression of metallothionein dismutases and reduced ROS levels.[126] This indicates that high WSS elicits a unique endothelial state—one that is neither distinctly atherogenic, nor representative of the quiescent baseline-WSS EC phenotype.

These newly identified EC responses under high WSS may be important for both adaptive and destructive remodeling. For example, the upregulated matrix degrading metalloproteinases (ADAMTS1, ADAMTS6) and serine proteases (tPA and uPA)[21] could facilitate IEL fragmentation in outward expansion, cap thinning in plaques, and massive matrix degradation (including IEL loss) in aneurysms. Indeed, uPA and ADAMTS1 proteins increased during outward remodeling of the basilar artery following bilateral CCA ligation,[21] while uPA and tPA are found in human IA tissue.[12]

Dolan *et al.* have also observed that high WSS values of 10 Pa[21] and 28.4 Pa[20] stimulate EC proliferation *in vitro*. This is consistent with earlier results by Metaxa *et al.*,[78] who found that cultured ECs in a tapered chamber, similar to that shown in Fig. 5a, increased proliferation as WSS increased from 2 to 10 Pa, and that this high-WSS stimulated proliferation was mediated by the nitric oxide pathway.[78] Interestingly, while Dolan *et al.*[20] found that the high proliferation was accompanied by high apoptosis in ECs experiencing high WSS of 28.4 Pa, Metaxa *et al.*[78] found that apoptosis decreased as WSS increased from 2 to 10 Pa. As we have previously suggested,[20] ECs may have bimodal responses to high WSS; there may be a threshold of high WSS at which WSS switches from being a eutrophic and protective signal to having detrimental effects (i.e., increased cell turnover) on ECs that may contribute to vascular pathology *in vivo*.

How ECs sense high WSS magnitudes is unclear. Any of the known EC sensing mechanisms under baseline or low WSS conditions could be involved in high WSS responses (i.e., glycocalyx, junction proteins, G proteins or their coupled receptors, ion channels, cytoskeleton, *etc.*[17]). Alternatively, EC responses could be modulated by sensors that are only activated under high WSS. One candidate is the stretch activated ion channel (SAC), which regulates calcium influx into ECs. The SAC inhibitor, streptomycin,

attenuated expansive remodeling of the flow-loaded CCA in mice.[108] While increased eNOS levels under high WSS (2.5–10 Pa) were attenuated by the inhibitor, eNOS protein in cultured ECs was unaffected by streptomycin at baseline WSS.[108] These results suggest that SACs are involved in high WSS sensing and remodeling.

Positive and Negative WSSG Elicit Distinct EC Responses

Although WSSG in the milieu of high WSS has been shown to contribute to IA formation and could play a role in atherosclerotic plaque instability, understanding of its effect on ECs is considerably lacking. *In vivo* studies indicate that aneurysmal damage initiates near the bifurcation apex with high WSS and positive WSSG, while downstream sections of the bifurcation experiencing equally high WSS but negative WSSG remain intact.[76, 79] This raises questions as to (1) if ECs are sensitive to WSSG, (2) if ECs can sense the sign of WSSG, and (3) what signaling pathways are triggered by these mechanical stimuli, leading to vastly different downstream outcomes (damaged vs. intact IEL under positive vs. negative WSSG).

To address these questions, newly designed *in vitro* flow loop systems have been utilized to study WSSG effect on EC biology in the milieu of high WSS.[20, 92, 105] Symanski *et al.* subjected cultured ECs to impinging flow in a T-shaped chamber designed to mimic an arterial bifurcation. They found that high WSS combined with positive WSSG caused ECs to migrate downstream of the impingement.[105] To obtain sufficient number of cells under constant WSSG and to separate the effects WSSG, Dolan *et al.*[20] built the system shown in Fig. 5b, to vary WSS between 3.5 and 28.4 Pa, in order to create positive WSSG (+980 Pa/m) and negative WSSG (21120 Pa/m), respectively. They found that ECs are able to distinguish the sign of WSSG, responding with vastly different cell alignment, proliferation, and apoptosis.[20] Positive WSSG inhibited while negative WSSG promoted flow-induced EC alignment (Fig. 5b). Sakamoto *et al.* also reported that ECs under high WSS and positive WSSG do not align nor develop prominent stress fibers.[92] Furthermore, Dolan *et al.*[20] found that proliferation and apoptosis were stimulated by positive WSSG and displayed similar response to ECs under 28.4 Pa without gradient. In contrast, proliferation and apoptosis were suppressed under negative WSSG and were similar to ECs under 3.5 Pa without gradient. Therefore it seems that WSSG can either exacerbate or ameliorate EC responses to high WSS depending on its sign.[20]

Inspired by the observed changes in ECs under WSSG, Dolan *et al.* subsequently studied gene expression differences between positive WSSG and negative WSSG under high WSS conditions (in review). Gene profiling of ECs revealed that cells under positive WSSG, as compared to negative WSSG, had higher mRNA expression of genes associated with proliferation, apoptosis and extracellular matrix processing while exhibiting decreased pro-inflammatory genes. Furthermore, similar responses occurred *in vivo* at the basilar terminus of rabbits undergoing bilateral carotid ligation to induce aneurysm formation.[27, 56, 74, 79] Both Ki-67, a marker of proliferating cells, and the metalloproteinase ADAMTS1 were higher in ECs under positive WSSG than in adjacent regions of negative WSSG. Overall these results indicate that ECs are sensitive to WSSG and are able to differentially respond to the sign of the gradient.

How WSSG induces changes in ECs is unknown. We believe that positive and negative WSSG represent two distinct mechanical stimuli on ECs as illustrated in Fig. 6. Positive WSSG (increasing WSS along the flow direction) creates a net stretching force along the apical surface of the endothelium,[61, 123] pulling cells apart (Fig. 6a). Negative WSSG causes net cell compression along the luminal surface, pressing cells together (Fig. 6b). Such shear gradient stretch/compression is not to be confused with the cyclic circumferential stretch of the vessel arising from pulsatile blood pressure.[17] First, these two types of stretches act in

orthogonal directions (as shown in Fig. 6), with the shear gradient stretch/compression being along the direction of flow and EC elongation. Second, while the effect of the cyclic stretch is felt by ECs because of their basal attachment to the distensible substrate (i.e., the vessel wall), the shear gradient stretch/compression is strictly acting from the luminal side of the endothelium.

Much has been learned about the combined effect of cyclic circumferential stretch and WSS, which can work synergistically on EC responses.[59, 81, 130] For example, alignment, stress fiber formation[81, 130] and Cx43[59] levels in ECs subjected to WSS are enhanced by the addition of cyclic stretch. However, little is known about the direct effect of the WSGG or the concomitant effects of WSS with WSSG. Based on our observations that positive WSSG exacerbated while negative WSSG ameliorated high WSS responses, we propose that WSSG may modulate WSS responses by adding to or subtracting from, respectively, the net stretch force already exerted *across* the endothelium by high WSS.[20]

The mechanosensory mechanism that allows ECs to respond specifically to WSSG is also unknown. Gradient may act on ECs by creating differences in WSS experienced by adjacent cells. These may act at intercellular junctions by preventing stable gap junction Cx43[19] and tight junction ZO-1[110] formation. Additionally, gradient may produce different conformations and/or different levels of activation in junction proteins such as PECAM-1, which is a part of a mechanosensory complex mediating EC responses to WSS.[117] A specific candidate has not yet been identified and warrants continued investigation.

The *in vitro* findings of the differential EC responses to positive, negative and no gradient provide a strong impetus to further investigate EC behavior under those WSS/WSSG conditions that contribute to vascular disease such as in IA initiation and stenotic plaque rupture. Our *in vivo* studies of aneurysm initiation[79] suggest that a threshold of WSS and WSSG may need to be reached before IEL damage and subsequent aneurysm formation can occur. Thus *in vitro* studies performed under such “above-threshold” hemodynamic conditions will shed light on the destructive mechanisms induced by ECs during pathological processes.

SUMMARY

High WSS (>3 Pa) has emerged as a key regulator of vascular biology and pathology, contributing to adaptive outward remodeling, pathological remodeling leading to saccular aneurysm initiation, and atherosclerotic plaque instability. Recent advances in IA pathogenesis using animal models have shed light on the role of high WSS in pathological remodeling, pointing to *high WSS in combination with positive WSSG* along the flow direction as the hemodynamic trigger for IA formation. Similar hemodynamic conditions also exist at the upstream throat of the stenosis, therefore prompting us to speculate a potential role of high WSS coupled with positive WSSG in plaque instability.

Given the overarching importance to better understand, predict and prevent aneurysm formation and plaque rupture, we are now beginning to elucidate EC function under these hemodynamic conditions, including high WSS alone or in combination with WSSG. Recent *in vitro* studies show that high WSS induces a gene expression profile indicative of an anti-inflammatory, anti-oxidative, proliferative, fibrinolytic and pro-matrix remodeling phenotype. Such EC responses do not recapitulate the known phenotype of quiescent ECs under baseline WSS, nor do they resemble the atherogenic phenotype of ECs under low WSS conditions. Furthermore, *in vitro* evidence confirms that ECs are not only sensitive to high WSS but also to the presence of WSSG and its sign. Positive WSSG appears to exacerbate EC responses to high WSS (e.g., increased apoptosis, proliferation and decreased alignment), while negative WSSG seems to ameliorate them. Candidate genes responsive to

positive WSSG may provide further insight into IA formation and plaque instability under the influence of flow.

Elucidating the effect of high WSS and WSSG on the endothelium and vascular pathobiology can pave the way for improving prediction of aneurysm development and plaque instability, guide intervention strategies, and identify molecular targets for pharmaceutical IA intervention and plaque stabilization and other disease that may associate with high WSS and positive WSSG.

Acknowledgments

We thank Nicholas Liaw for critical review of the manuscript and assistance with figures, and Chris Martensen for assistance with figures and references. This work was supported by NIH grant R01NS064592 (awarded to H.M.).

REFERENCES

1. Abruzzo T, Kendler A, Apkarian R, Workman M, Khoury JC, Cloft HJ. Cerebral aneurysm formation in nitric oxide synthase-3 knockout mice. Curr. Neurovasc. Res. 2007; 4:161–169. [PubMed: 17691969]
2. Alnaes MS, Isaksen J, Mardal KA, Romner B, Morgan MK, Ingebrigtsen T. Computation of hemodynamics in the circle of Willis. Stroke. 2007; 38:2500–2505. [PubMed: 17673714]
3. Aoki T, Kataoka H, Ishibashi R, Nozaki K, Egashira K, Hashimoto N. Impact of monocyte chemoattractant protein-1 deficiency on cerebral aneurysm formation. Stroke. 2009; 40:942–951. [PubMed: 19164781]
4. Aoki T, Kataoka H, Ishibashi R, Nozaki K, Hashimoto N. Cathepsin B, K, and S are expressed in cerebral aneurysms and promote the progression of cerebral aneurysms. Stroke. 2008; 39:2603–2610. [PubMed: 18635848]
5. Aoki T, Kataoka H, Morimoto M, Nozaki K, Hashimoto N. Macrophage-derived matrix metalloproteinase-2 and-9 promote the progression of cerebral aneurysms in rats. Stroke. 2007; 38:162–169. [PubMed: 17122420]
6. Aoki T, Kataoka H, Nishimura M, Ishibashi R, Morishita R, Miyamoto S. Ets-1 promotes the progression of cerebral aneurysm by inducing the expression of MCP-1 in vascular smooth muscle cells. Gene Ther. 2010; 17:1117–1123. [PubMed: 20428211]
7. Aoki T, Kataoka H, Shimamura M, Nakagami H, Wakayama K, Moriwaki T, Ishibashi R, Nozaki K, Morishita R, Hashimoto N. NF-kappaB is a key mediator of cerebral aneurysm formation. Circulation. 2007; 116:2830–2840. [PubMed: 18025535]
8. Aoki T, Nishimura M, Kataoka H, Ishibashi R, Nozaki K, Miyamoto S. Complementary inhibition of cerebral aneurysm formation by eNOS and nNOS. Lab. Invest. 2011; 91:619–626. [PubMed: 21321533]
9. Aoki T, Nishimura M, Matsuoka T, Yamamoto K, Furuyashiki T, Kataoka H, Kitaoka S, Ishibashi R, Ishibazawa A, Miyamoto S, Morishita R, Ando J, Hashimoto N, Nozaki K, Narumiya S. PGE(2) -EP(2) signalling in endothelium is activated by haemodynamic stress and induces cerebral aneurysm through an amplifying loop *via* NF-kappaB. Br. J. Pharmacol. 2011; 163:1237–1249. [PubMed: 21426319]
10. Bark DL Jr, Para AN, Ku DN. Correlation of thrombosis growth rate to pathological wall shear rate during platelet accumulation. Biotechnol. Bioeng. 2012; 109:2642–2650. [PubMed: 22539078]
11. Brown RD Jr, Wiebers DO, Forbes GS. Unruptured intracranial aneurysms and arteriovenous malformations: frequency of intracranial hemorrhage and relationship of lesions. J Neurosurg. 1990; 73:859–863. [PubMed: 2230969]
12. Bruno G, Todor R, Lewis I, Chyatte D. Vascular extracellular matrix remodeling in cerebral aneurysms. J Neurosurg. 1998; 89:431–440. [PubMed: 9724118]
13. Burke A, Fitzgerald GA. Oxidative stress and smoking-induced vascular injury. Prog. Cardiovasc. Dis. 2003; 46:79–90. [PubMed: 12920701]

14. Caro CG, Fitz-Gerald JM, Schroter RC. Atheroma and arterial wall shear. Observation, correlation and proposal of a shear dependent mass transfer mechanism for atherogenesis. Proc. R. Soc. Lond. B Biol. Sci. 1971; 177:109–159. [PubMed: 4396262]
15. Castier Y, Brandes RP, Leseche G, Tedgui A, Lehoux S. p47phox-dependent NADPH oxidase regulates flow-induced vascular remodeling. Circ. Res. 2005; 97:533–540. [PubMed: 16109921]
16. Chatzizisis YS, Jonas M, Coskun AU, Beigel R, Stone BV, Maynard C, Gerrity RG, Daley W, Rogers C, Edelman ER, Feldman CL, Stone PH. Prediction of the localization of high-risk coronary atherosclerotic plaques on the basis of low endothelial shear stress: an intravascular ultrasound and histopathology natural history study. Circulation. 2008; 117:993–1002. [PubMed: 18250270]
17. Chien S. Mechanotransduction and endothelial cell homeostasis: the wisdom of the cell. Am. J. Physiol. Heart Circ. Physiol. 2007; 292:H1209–H1224. [PubMed: 17098825]
18. Davies PF. Flow-mediated endothelial mechanotransduction. Physiol. Rev. 1995; 75:519–560. [PubMed: 7624393]
19. DePaola N, Davies PF, Pritchard WF Jr, Florez L, Harbeck N, Polacek DC. Spatial and temporal regulation of gap junction connexin43 in vascular endothelial cells exposed to controlled disturbed flows in vitro. Proc. Natl Acad. Sci. USA. 1999; 96:3154–3159. [PubMed: 10077653]
20. Dolan JM, Meng H, Singh S, Paluch R, Kolega J. High fluid shear stress and spatial shear stress gradients affect endothelial proliferation, survival, and alignment. Ann. Biomed. Eng. 2011; 39:1620–1631. [PubMed: 21312062]
21. Dolan JM, Sim FJ, Meng H, Kolega J. Endothelial cells express a unique transcriptional profile under very high wall shear stress known to induce expansive arterial remodeling. Am. J. Physiol. Cell Physiol. 2012; 302:C1109–C1118. [PubMed: 22173868]
22. Dumont O, Loufrani L, Henrion D. Key role of the NO-pathway and matrix metalloprotease-9 in high blood flow-induced remodeling of rat resistance arteries. Arterioscler. Thromb. Vasc. Biol. 2007; 27:317–324. [PubMed: 17158349]
23. Eldawoody H, Shimizu H, Kimura N, Saito A, Nakayama T, Takahashi A, Tominaga T. Simplified experimental cerebral aneurysm model in rats: comprehensive evaluation of induced aneurysms and arterial changes in the circle of Willis. Brain Res. 2009; 1300:159–168. [PubMed: 19747458]
24. Frosen J, Tulamo R, Paetau A, Laaksamo E, Korja M, Laakso A, Niemela M, Hernesniemi J. Saccular intracranial aneurysm: pathology and mechanisms. Acta Neuropathol. 2012; 123:773–786. [PubMed: 22249619]
25. Fujii K, Kobayashi Y, Mintz GS, Takebayashi H, Dangas G, Moussa I, Mehran R, Lansky AJ, Kreps E, Collins M, Colombo A, Stone GW, Leon MB, Moses JW. Intravascular ultrasound assessment of ulcerated ruptured plaques: a comparison of culprit and nonculprit lesions of patients with acute coronary syndromes and lesions in patients without acute coronary syndromes. Circulation. 2003; 108:2473–2478. [PubMed: 14610010]
26. Fukuda S, Hashimoto N, Naritomi H, Nagata I, Nozaki K, Kondo S, Kurino M, Kikuchi H. Prevention of rat cerebral aneurysm formation by inhibition of nitric oxide synthase. Circulation. 2000; 101:2532–2538. [PubMed: 10831529]
27. Gao L, Hoi Y, Swartz DD, Kolega J, Siddiqui A, Meng H. Nascent aneurysm formation at the basilar terminus induced by hemodynamics. Stroke. 2008; 39:2085–2090. [PubMed: 18451348]
28. Gertz SD, Roberts WC. Hemodynamic shear force in rupture of coronary arterial atherosclerotic plaques. Am. J. Cardiol. 1990; 66:1368–1372. [PubMed: 2244569]
29. Gibbons GH, Dzau VJ. The emerging concept of vascular remodeling. N. Engl. J. Med. 1994; 330:1431–1438. [PubMed: 8159199]
30. Gijsen FJ, Mastik F, Schaar JA, Schuurbiers JC, van der Giessen WJ, de Feyter PJ, Serruys PW, van der Steen AF, Wentzel JJ. High shear stress induces a strain increase in human coronary plaques over a 6- month period. EuroIntervention. 2011; 7:121–127. [PubMed: 21550912]
31. Gijsen FJ, Wentzel JJ, Thury A, Mastik F, Schaar JA, Schuurbiers JC, Slager CJ, van der Giessen WJ, de Feyter PJ, van der Steen AF, Serruys PW. Strain distribution over plaques in human coronary arteries relates to shear stress. Am. J. Physiol. Heart Circ. Physiol. 2008; 295:H1608–H1614. [PubMed: 18621851]

32. Glagov S, Weisenberg E, Zarins CK, Stankunavicius R, Kolettis GJ. Compensatory enlargement of human atherosclerotic coronary arteries. N. Engl. J. Med. 1987; 316:1371–1375. [PubMed: 3574413]
33. Glagov S, Zarins C, Giddens DP, Ku DN. Hemodynamics and atherosclerosis. Insights and perspectives gained from studies of human arteries. Arch. Pathol. Lab. Med. 1988; 112:1018–1031. [PubMed: 3052352]
34. Greve JM, Les AS, Tang BT, Draney Blomme MT, Wilson NM, Dalman RL, Pelc NJ, Taylor CA. Allometric scaling of wall shear stress from mice to humans: quantification using cine phase-contrast MRI and computational fluid dynamics. Am. J. Physiol. Heart Circ. Physiol. 2006; 291:H1700–H1708. [PubMed: 16714362]
35. Groen HC, Gijsen FJ, van der Lugt A, Ferguson MS, Hatsukami TS, van der Steen AF, Yuan C, Wentzel JJ. Plaque rupture in the carotid artery is localized at the high shear stress region: a case report. Stroke. 2007; 38:2379–2381. [PubMed: 17615365]
36. Guzman RJ, Abe K, Zarins CK. Flow-induced arterial enlargement is inhibited by suppression of nitric oxide synthase activity in vivo. Surgery. 1997; 122:273–279. discussion 279–280. [PubMed: 9288132]
37. Han HC. Twisted blood vessels: symptoms, etiology and biomechanical mechanisms. J Vasc. Res. 2012; 49:185–197. [PubMed: 22433458]
38. Hashimoto N, Handa H, Hazama F. Experimentally induced cerebral aneurysms in rats. Surg. Neurol. 1978; 10:3–8. [PubMed: 684603]
39. Hashimoto N, Handa H, Nagata I, Hazama F. Experimentally induced cerebral aneurysms in rats: Part V. Relation of hemodynamics in the circle of Willis to formation of aneurysms. Surg. Neurol. 1980; 13:41–45. [PubMed: 7361257]
40. Hashimoto T, Meng H, Young WL. Intracranial aneurysms: links among inflammation, hemodynamics and vascular remodeling. Neurol. Res. 2006; 28:372–380. [PubMed: 16759441]
41. Hazama F, Kataoka H, Yamada E, Kayembe K, Hashimoto N, Kojima M, Kim C. Early changes of experimentally induced cerebral aneurysms in rats. Lightmicroscopic study. Am. J. Pathol. 1986; 124:399–404. [PubMed: 3766700]
42. Hoi Y, Gao L, Tremmel M, Paluch RA, Siddiqui AH, Meng H, Mocco J. In vivo assessment of rapid cerebrovascular morphological adaptation following acute blood flow increase. J Neurosurg. 2008; 109:1141–1147. [PubMed: 19035734]
43. Hsieh HJ, Li NQ, Frangos JA. Shear-induced platelet-derived growth factor gene expression in human endothelial cells is mediated by protein kinase C. J Cell. Physiol. 1992; 150:552–558. [PubMed: 1537884]
44. Hyun S, Kleinstreuer C, Archie JP Jr. Hemodynamics analyses of arterial expansions with implications to thrombosis and restenosis. Med. Eng. Phys. 2000; 22:13–27. [PubMed: 10817945]
45. Ishibashi A, Yokokura Y, Kojima K, Abe T. Acute obstructive hydrocephalus due to an unruptured basilar bifurcation aneurysm associated with bilateral internal carotid occlusion—a case report. Kurume Med. J. 1993; 40:21–25. [PubMed: 8355475]
46. Jamous MA, Nagahiro S, Kitazato KT, Satomi J, Satoh K. Role of estrogen deficiency in the formation and progression of cerebral aneurysms. Part I: experimental study of the effect of oophorectomy in rats. J Neurosurg. 2005; 103:1046–1051. [PubMed: 16381191]
47. Jamous MA, Nagahiro S, Kitazato KT, Tamura T, Aziz HA, Shono M, Satoh K. Endothelial injury and inflammatory response induced by hemodynamic changes preceding intracranial aneurysm formation: experimental study in rats. J Neurosurg. 2007; 107:405–411. [PubMed: 17695397]
48. Jesty J, Yin W, Perrotta P, Bluestein D. Platelet activation in a circulating flow loop: combined effects of shear stress and exposure time. Platelets. 2003; 14:143–149. [PubMed: 12850838]
49. Jou LD, van Tyen R, Berger SA, Saloner D. Calculation of the magnetization distribution for fluid flow in curved vessels. Magn. Reson. Med. 1996; 35:577–584. [PubMed: 8992209]
50. Juvela S. Natural history of unruptured intracranial aneurysms: risks for aneurysm formation, growth, and rupture. Acta Neurochir. Suppl. 2002; 82:27–30. [PubMed: 12378985]
51. Kamiya A, Bukhari R, Togawa T. Adaptive regulation of wall shear stress optimizing vascular tree function. Bull. Math. Biol. 1984; 46:127–137. [PubMed: 6713148]

52. Kamiya A, Togawa T. Adaptive regulation of wall shear stress to flow change in the canine carotid artery. Am. J. Physiol. 1980; 239:H14–H21. [PubMed: 7396013]
53. Karwowski JK, Markezich A, Whitson J, Abbruzzese TA, Zarins CK, Dalman RL. Dosedependent limitation of arterial enlargement by the matrix metalloproteinase inhibitor RS-113,456. J Surg. Res. 1999; 87:122–129. [PubMed: 10527713]
54. Kataoka K, Taneda M, Asai T, Kinoshita A, Ito M, Kuroda R. Structural fragility and inflammatory response of ruptured cerebral aneurysms. A comparative study between ruptured and unruptured cerebral aneurysms. Stroke. 1999; 30:1396–1401. [PubMed: 10390313]
55. Kojima M, Handa H, Hashimoto N, Kim C, Hazama F. Early changes of experimentally induced cerebral aneurysms in rats: scanning electron microscopic study. Stroke. 1986; 17:835–841. [PubMed: 3764951]
56. Kolega J, Gao L, Mandelbaum M, Mocco J, Siddiqui AH, Natarajan SK, Meng H. Cellular and molecular responses of the basilar terminus to hemodynamics during intracranial aneurysm initiation in a rabbit model. J Vasc. Res. 2011; 48:429–442. [PubMed: 21625176]
57. Koskinas KC, Feldman CL, Chatzizisis YS, Coskun AU, Jonas M, Maynard C, Baker AB, Papafaklis MI, Edelman ER, Stone PH. Natural history of experimental coronary atherosclerosis and vascular remodeling in relation to endothelial shear stress: a serial, in vivo intravascular ultrasound study. Circulation. 2010; 121:2092–2101. [PubMed: 20439786]
58. Kulcsar Z, Ugron A, Marosfoi M, Berentei Z, Paal G, Szikora I. Hemodynamics of cerebral aneurysm initiation: the role of wall shear stress and spatial wall shear stress gradient. AJNR Am. J. Neuroradiol. 2011; 32:587–594. [PubMed: 21310860]
59. Kwak BR, Silacci P, Stergiopulos N, Hayoz D, Meda P. Shear stress and cyclic circumferential stretch, but not pressure, alter connexin43 expression in endothelial cells. Cell Commun. Adhes. 2005; 12:261–270. [PubMed: 16531321]
60. LaBarbera M. Principles of design of fluid transport systems in zoology. Science. 1990; 249:992–1000. [PubMed: 2396104]
61. LaMack JA, Friedman MH. Individual and combined effects of shear stress magnitude and spatial gradient on endothelial cell gene expression. Am. J. Physiol. Heart Circ. Physiol. 2007; 293:H2853–H2859. [PubMed: 17766484]
62. Langille BL, O'Donnell F. Reductions in arterial diameter produced by chronic decreases in blood flow are endothelium-dependent. Science. 1986; 231:405–407. [PubMed: 3941904]
63. Leach JR, Rayz VL, Soares B, Wintermark M, Mofrad MR, Saloner D. Carotid atheroma rupture observed in vivo and FSI-predicted stress distribution based on pre-rupture imaging. Ann. Biomed. Eng. 2010; 38:2748–2765. [PubMed: 20232151]
64. Lehman RM, Owens GK, Kassell NF, Hongo K. Mechanism of enlargement of major cerebral collateral arteries in rabbits. Stroke. 1991; 22:499–504. [PubMed: 2024279]
65. Lehoux S, Castier Y, Tedgui A. Molecular mechanisms of the vascular responses to haemodynamic forces. J Intern. Med. 2006; 259:381–392. [PubMed: 16594906]
66. Lehoux S, Tronc F, Tedgui A. Mechanisms of blood flow-induced vascular enlargement. Biorheology. 2002; 39:319–324. [PubMed: 12122247]
67. Levkau B, Kenagy RD, Karsan A, Weitkamp B, Clowes AW, Ross R, Raines EW. Activation of metalloproteinases and their association with integrins: an auxiliary apoptotic pathway in human endothelial cells. Cell Death Differ. 2002; 9:1360–1367. [PubMed: 12478473]
68. Li ZY, Taviani V, Tang T, Sadat U, Young V, Patterson A, Graves M, Gillard JH. The mechanical triggers of plaque rupture: shear stress vs pressure gradient. Br. J. Radiol. 2009; 82(Spec No. 1):S39–S45. [PubMed: 20348535]
69. Lindekleiv HM, Valen-Sendstad K, Morgan MK, Mardal KA, Faulder K, Magnus JH, Waterloo K, Romner B, Ingebrigtsen T. Sex differences in intracranial arterial bifurcations. Gend. Med. 2010; 7:149–155. [PubMed: 20435277]
70. Lovett JK, Rothwell PM. Site of carotid plaque ulceration in relation to direction of blood flow: an angiographic and pathological study. Cerebrovasc. Dis. 2003; 16:369–375. [PubMed: 13130178]
71. Malek AM, Alper SL, Izumo S. Hemodynamic shear stress and its role in atherosclerosis. JAMA. 1999; 282:2035–2042. [PubMed: 10591386]

72. Malek AM, Gibbons GH, Dzau VJ, Izumo S. Fluid shear stress differentially modulates expression of genes encoding basic fibroblast growth factor and platelet- derived growth factor B chain in vascular endothelium. J Clin. Invest. 1993; 92:2013–2021. [PubMed: 8408655]
73. Masuda H, Zhuang YJ, Singh TM, Kawamura K, Murakami M, Zarins CK, Glagov S. Adaptive remodeling of internal elastic lamina and endothelial lining during flow-induced arterial enlargement. Arterioscler. Thromb. Vasc. Biol. 1999; 19:2298–2307. [PubMed: 10521357]
74. Meng H, Metaxa E, Gao L, Liaw N, Natarajan SK, Swartz DD, Siddiqui AH, Kolega J, Mocco J. Progressive aneurysm development following hemodynamic insult. J Neurosurg. 2011; 114:1095–1103. [PubMed: 20950086]
75. Meng H, Swartz DD, Wang Z, Hoi Y, Kolega J, Metaxa EM, Szymanski MP, Yamamoto J, Sauvageau E, Levy EI. A model system for mapping vascular responses to complex hemodynamics at arterial bifurcations in vivo. Neurosurgery. 2006; 59:1094–1100. discussion 1100–1101. [PubMed: 17143243]
76. Meng H, Wang Z, Hoi Y, Gao L, Metaxa E, Swartz DD, Kolega J. Complex hemodynamics at the apex of an arterial bifurcation induces vascular remodeling resembling cerebral aneurysm initiation. Stroke. 2007; 38:1924–1931. [PubMed: 17495215]
77. Meng H, Xiang J, Liaw N. The role of hemodynamics in intracranial aneurysm initiation. Int. Rev. Thrombosis. 2012; 7:40–57.
78. Metaxa E, Meng H, Kaluvala SR, Szymanski MP, Paluch RA, Kolega J. Nitric oxide-dependent stimulation of endothelial cell proliferation by sustained high flow. Am. J. Physiol. Heart Circ. Physiol. 2008; 295:H736–H742. [PubMed: 18552158]
79. Metaxa E, Tremmel M, Natarajan SK, Xiang J, Paluch RA, Mandelbaum M, Siddiqui AH, Kolega J, Mocco J, Meng H. Characterization of critical hemodynamics contributing to aneurysmal remodeling at the basilar terminus in a rabbit model. Stroke. 2010; 41:1774–1782. [PubMed: 20595660]
80. Mintz GS, Kent KM, Pichard AD, Satler LF, Popma JJ, Leon MB. Contribution of inadequate arterial remodeling to the development of focal coronary artery stenoses. An intravascular ultrasound study. Circulation. 1997; 95:1791–1798. [PubMed: 9107165]
81. Moore JE Jr, Burki E, Suciu A, Zhao S, Burnier M, Brunner HR, Meister JJ. A device for subjecting vascular endothelial cells to both fluid shear stress and circumferential cyclic stretch. Ann. Biomed. Eng. 1994; 22:416–422. [PubMed: 7998687]
82. Moriwaki T, Takagi Y, Sadamasa N, Aoki T, Nozaki K, Hashimoto N. Impaired progression of cerebral aneurysms in interleukin-1beta-deficient mice. Stroke. 2006; 37:900–905. [PubMed: 16439700]
83. Murray CD. The physiological principle of minimum work: I. The vascular system and the cost of blood volume. Proc. Natl Acad. Sci. USA. 1926; 12:207–214. [PubMed: 16576980]
84. Nagata I, Handa H, Hashimoto N, Hazama F. Experimentally induced cerebral aneurysms in rats: Part VI. Hypertension. Surg. Neurol. 1980; 14:477–479. [PubMed: 6111849]
85. Nakatani H, Hashimoto N, Kang Y, Yamazoe N, Kikuchi H, Yamaguchi S, Niimi H. Cerebral blood flow patterns at major vessel bifurcations and aneurysms in rats. J Neurosurg. 1991; 74:258–262. [PubMed: 1988596]
86. Neelamegham S, Taylor AD, Burns AR, Smith CW, Simon SI. Hydrodynamic shear shows distinct roles for LFA-1 and Mac-1 in neutrophil adhesion to intercellular adhesion molecule-1. Blood. 1998; 92:1626–1638. [PubMed: 9716590]
87. Nuki Y, Matsumoto MM, Tsang E, Young WL, van Rooijen N, Kurihara C, Hashimoto T. Roles of macrophages in flow-induced outward vascular remodeling. J Cereb. Blood Flow Metab. 2009; 29:495–503. [PubMed: 19002198]
88. Park JB, Charbonneau F, Schiffrin EL. Correlation of endothelial function in large and small arteries in human essential hypertension. J Hypertens. 2001; 19:415–420. [PubMed: 11288811]
89. Rajagopalan S, Meng XP, Ramasamy S, Harrison DG, Galis ZS. Reactive oxygen species produced by macrophage-derived foam cells regulate the activity of vascular matrix metalloproteinases in vitro. Implications for atherosclerotic plaque stability. J Clin. Invest. 1996; 98:2572–2579. [PubMed: 8958220]

90. Rinkel GJ, Djibuti M, Algra A, van Gijn J. Prevalence and risk of rupture of intracranial aneurysms: a systematic review. Stroke. 1998; 29:251–256. [PubMed: 9445359]
91. Ross R. Atherosclerosis—an inflammatory disease. N. Engl. J. Med. 1999; 340:115–126. [PubMed: 9887164]
92. Sakamoto N, Saito N, Han X, Ohashi T, Sato M. Effect of spatial gradient in fluid shear stress on morphological changes in endothelial cells in response to flow. Biochem. Biophys. Res. Commun. 2010; 395:264–269. [PubMed: 20371223]
93. Samady H, Eshtehardi P, McDaniel MC, Suo J, Dhawan SS, Maynard C, Timmins LH, Quyyumi AA, Giddens DP. Coronary artery wall shear stress is associated with progression and transformation of atherosclerotic plaque and arterial remodeling in patients with coronary artery disease. Circulation. 2011; 124:779–788. [PubMed: 21788584]
94. Schiffrin EL, Park JB, Intengan HD, Touyz RM. Correction of arterial structure and endothelial dysfunction in human essential hypertension by the angiotensin receptor antagonist losartan. Circulation. 2000; 101:1653–1659. [PubMed: 10758046]
95. Schirmer CM, Malek AM. Computational fluid dynamic characterization of carotid bifurcation stenosis in patient-based geometries. Brain Behav. 2012; 2:42–52. [PubMed: 22574273]
96. Schirmer CM, Malek AM. Wall shear stress gradient analysis within an idealized stenosis using non- Newtonian flow. Neurosurgery. 2007; 61:853–863. discussion 863–864. [PubMed: 17986948]
97. Schoenhagen P, Ziada KM, Kapadia SR, Crowe TD, Nissen SE, Tuzcu EM. Extent and direction of arterial remodeling in stable versus unstable coronary syndromes : an intravascular ultrasound study. Circulation. 2000; 101:598–603. [PubMed: 10673250]
98. Sho E, Komatsu M, Sho M, Nanjo H, Singh TM, Xu C, Masuda H, Zarins CK. High flow drives vascular endothelial cell proliferation during flow-induced arterial remodeling associated with the expression of vascular endothelial growth factor. Exp. Mol. Pathol. 2003; 75:1–11. [PubMed: 12834620]
99. Sho E, Sho M, Singh TM, Nanjo H, Komatsu M, Xu C, Masuda H, Zarins CK. Arterial enlargement in response to high flow requires early expression of matrix metalloproteinases to degrade extracellular matrix. Exp. Mol. Pathol. 2002; 73:142–153. [PubMed: 12231217]
100. Shumacker HB Jr. Aneurysm development and degenerative changes in dilated artery proximal to arteriovenous fistula. Surg. Gynecol. Obstet. 1970; 130:636–640. [PubMed: 5436601]
101. Singh TM, Abe KY, Sasaki T, Zhuang YJ, Masuda H, Zarins CK. Basic fibroblast growth factor expression precedes flow-induced arterial enlargement. J Surg. Res. 1998; 77:165–173. [PubMed: 9733604]
102. Slager CJ, Wentzel JJ, Gijsen FJ, Schuurbiers JC, van der Wal AC, van der Steen AF, Serruys PW. The role of shear stress in the generation of rupture-prone vulnerable plaques. Nat. Clin. Pract. Cardiovasc. Med. 2005; 2:401–407. [PubMed: 16119702]
103. Stehbens WE. Aneurysms and anatomical variation of cerebral arteries. Arch. Pathol. 1963; 75:45–64. [PubMed: 14087271]
104. Stone PH, Coskun AU, Kinlay S, Clark ME, Sonka M, Wahle A, Ilegbusi OJ, Yeghiazarians Y, Popma JJ, Orav J, Kuntz RE, Feldman CL. Effect of endothelial shear stress on the progression of coronary artery disease, vascular remodeling, and in-stent restenosis in humans: in vivo 6-month follow-up study. Circulation. 2003; 108:438–444. [PubMed: 12860915]
105. Szymanski MP, Metaxa E, Meng H, Kolega J. Endothelial cell layer subjected to impinging flow mimicking the apex of an arterial bifurcation. Ann. Biomed. Eng. 2008; 36:1681–1689. [PubMed: 18654851]
106. Tada Y, Kitazato KT, Yagi K, Shimada K, Matsushita N, Kinouchi T, Kanematsu Y, Satomi J, Kageji T, Nagahiro S. Statins promote the growth of experimentally induced cerebral aneurysms in estrogendeficient rats. Stroke. 2011; 42:2286–2293. [PubMed: 21737796]
107. Tada Y, Yagi K, Kitazato KT, Tamura T, Kinouchi T, Shimada K, Matsushita N, Nakajima N, Satomi J, Kageji T, Nagahiro S. Reduction of endothelial tight junction proteins is related to cerebral aneurysm formation in rats. J Hypertens. 2010; 28:1883–1891. [PubMed: 20577123]

108. Tanweer O, Metaxa E, Liaw N, Sternberg S, Siddiqui A, Kolega J, Meng H. Inhibition of stretch-activated ion channels on endothelial cells disrupts nitric oxide-mediated arterial outward remodeling. J Biorheol. 2011; 24:77–83.
109. Teng Z, Canton G, Yuan C, Ferguson M, Yang C, Huang X, Zheng J, Woodard PK, Tang D. 3D critical plaque wall stress is a better predictor of carotid plaque rupture sites than flow shear stress: an in vivo MRIbased 3D FSI study. J Biomech. Eng. 2010; 132:031007. [PubMed: 20459195]
110. Thi MM, Tarbell JM, Weinbaum S, Spray DC. The role of the glycocalyx in reorganization of the actin cytoskeleton under fluid shear stress: a “bumper-car” model. Proc. Natl Acad. Sci. USA. 2004; 101:16483–16488. [PubMed: 15545600]
111. Tohda K, Masuda H, Kawamura K, Shozawa T. Difference in dilatation between endothelium-preserved and -desquamated segments in the flow-loaded rat common carotid artery. Arterioscler. Thromb. 1992; 12:519–528. [PubMed: 1558839]
112. Torii R, Wood NB, Hadjiloizou N, Dowsey AW, Wright AR, Hughes AD, Davies J, Francis DP, Mayet J, Yang GZ, Thom SA, Xu XY. Stress phase angle depicts differences in coronary artery hemodynamics due to changes in flow and geometry after percutaneous coronary intervention. Am. J. Physiol. Heart Circ. Physiol. 2009; 296:H765–H776. [PubMed: 19151251]
113. Tremmel M, Xiang J, Natarajan SK, Hopkins LN, Siddiqui AH, Levy EI, Meng H. Alteration of intra-aneurysmal hemodynamics for flow diversion using enterprise and vision stents. World Neurosurg. 2010; 74:306–315. [PubMed: 21197155]
114. Tronc F, Mallat Z, Lehoux S, Wassef M, Esposito B, Tedgui A. Role of matrix metalloproteinases in blood flow-induced arterial enlargement: interaction with NO. Arterioscler. Thromb. Vasc. Biol. 2000; 20:E120–E126. [PubMed: 11116076]
115. Tronc F, Wassef M, Esposito B, Henrion D, Glagov S, Tedgui A. Role of NO in flow-induced remodeling of the rabbit common carotid artery. Arterioscler. Thromb. Vasc. Biol. 1996; 16:1256–1262. [PubMed: 8857922]
116. Tuttle JL, Nachreiner RD, Bhuller AS, Condict KW, Connors BA, Herring BP, Dalsing MC, Unthank JL. Shear level influences resistance artery remodeling: wall dimensions, cell density, and eNOS expression. Am. J. Physiol. Heart Circ. Physiol. 2001; 281:H1380–H1389. [PubMed: 11514310]
117. Tzima E, Irani-Tehrani M, Kiosses WB, Dejana E, Schultz DA, Engelhardt B, Cao G, DeLisser H, Schwartz MA. A mechanosensory complex that mediates the endothelial cell response to fluid shear stress. Nature. 2005; 437:426–431. [PubMed: 16163360]
118. van Everdingen KJ, Klijn CJ, Kappelle LJ, Mali WP, van der Grond J. MRA flow quantification in patients with a symptomatic internal carotid artery occlusion. The Dutch EC-IC Bypass Study Group. Stroke. 1997; 28:1595–1600. [PubMed: 9259755]
119. Van Remmen H, Williams MD, Guo Z, Estlack L, Yang H, Carlson EJ, Epstein CJ, Huang TT, Richardson A. Knockout mice heterozygous for Sod2 show alterations in cardiac mitochondrial function and apoptosis. Am. J. Physiol. Heart Circ. Physiol. 2001; 281:H1422–H1432. [PubMed: 11514315]
120. Varnava AM, Mills PG, Davies MJ. Relationship between coronary artery remodeling and plaque vulnerability. Circulation. 2002; 105:939–943. [PubMed: 11864922]
121. Vega C, Kwoon JV, Lavine SD. Intracranial aneurysms: current evidence and clinical practice. Am. Fam. Physician. 2002; 66:601–608. [PubMed: 12201551]
122. Waga S, Okada M, Kojima T. Saccular aneurysm associated with absence of the left cervical carotid arteries. Neurosurgery. 1978; 3:208–212. [PubMed: 703939]
123. Wang Z, Kolega J, Hoi Y, Gao L, Swartz DD, Levy EI, Mocco J, Meng H. Molecular alterations associated with aneurysmal remodeling are localized in the high hemodynamic stress region of a created carotid bifurcation. Neurosurgery. 2009; 65:169–177. discussion 177–178. [PubMed: 19574839]
124. Weinberg PD, Ross Ethier C. Twenty-fold difference in hemodynamic wall shear stress between murine and human aortas. J Biomech. 2007; 40:1594–1598. [PubMed: 17046000]
125. Wentzel JJ, Chatzizisis YS, Gijsen FJ, Giannoglou GD, Feldman CL, Stone PH. Endothelial shear stress in the evolution of coronary atherosclerotic plaque and vascular remodeling: current

understanding and remaining questions. Cardiovasc. Res. 2012; 96(2):234–243. [PubMed: 22752349]

126. White SJ, Hayes EM, Lehoux S, Jeremy JY, Horrevoets AJ, Newby AC. Characterization of the differential response of endothelial cells exposed to normal and elevated laminar shear stress. J Cell. Physiol. 2011; 226:2841–2848. [PubMed: 21302282]
127. Yong-Zhong G, van Alphen HA. Pathogenesis and histopathology of saccular aneurysms: review of the literature. Neurol. Res. 1990; 12:249–255. [PubMed: 1982169]
128. Zarins CK, Giddens DP, Bharadvaj BK, Sottiurai VS, Mabon RF, Glagov S. Carotid bifurcation atherosclerosis. Quantitative correlation of plaque localization with flow velocity profiles and wall shear stress. Circ. Res. 1983; 53:502–514. [PubMed: 6627609]
129. Zarins CK, Zatina MA, Giddens DP, Ku DN, Glagov S. Shear stress regulation of artery lumen diameter in experimental atherogenesis. J Vasc. Surg. 1987; 5:413–420. [PubMed: 3509594]
130. Zhao S, Suciu A, Ziegler T, Moore JE Jr, Burki E, Meister JJ, Brunner HR. Synergistic effects of fluid shear stress and cyclic circumferential stretch on vascular endothelial cell morphology and cytoskeleton. Arterioscler. Thromb. Vasc. Biol. 1995; 15:1781–1786. [PubMed: 7583556]

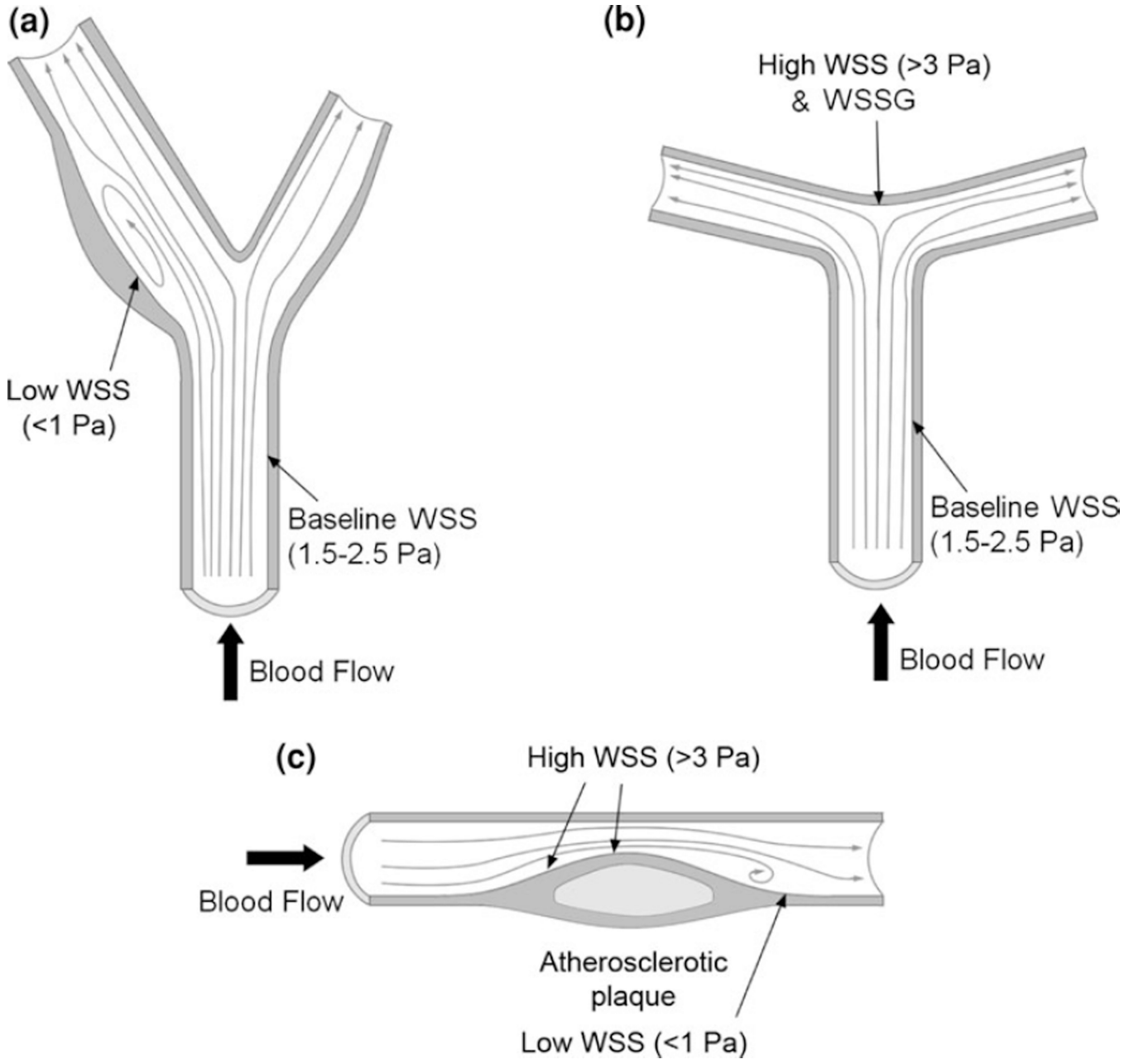

FIGURE 1.

Examples of arterial geometries with different WSS characteristics. (a) Carotid bifurcation with disturbed flow in the sinus opposite the apex, characterized by low WSS, and prone to atherogenesis. (b) Cerebral bifurcation with apex experiencing high WSS and WSSG resulting from flow impingement are prone to aneurysm formation. (c) Arterial stenosis, with both high WSS (upstream shoulder) and low WSS (downstream, disturbed flow).

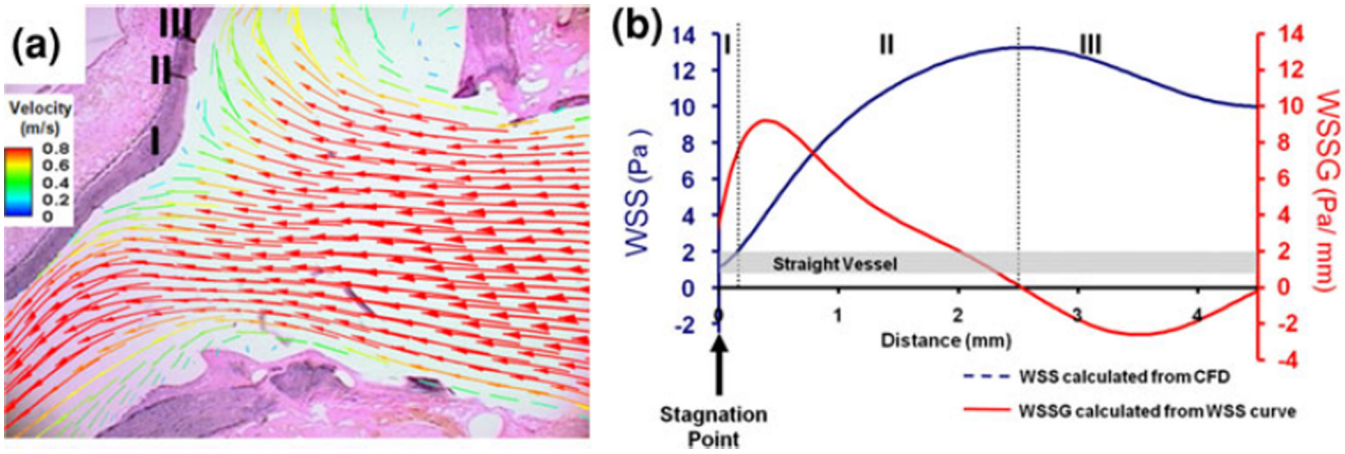

FIGURE 2.

Hemodynamic-histology co-mapping in the canine *de novo* bifurcation model reveals specific hemodynamic conditions leading to different remodeling responses. (a) Overlay of flow velocity vectors on the corresponding histological section. (b) Plot of WSS (blue) and WSSG (red) vs. distance from the apex revealing 3 regions with distinct flow patterns and remodeling responses from (a). Region 1: the impingement region with hyperplastic responses; Region II: acceleration region with aneurysmlike remodeling; and Region III: decelerating flow and recovery to baseline flow with no morphological changes. From Meng *et al.*[76] Reproduced with permission.

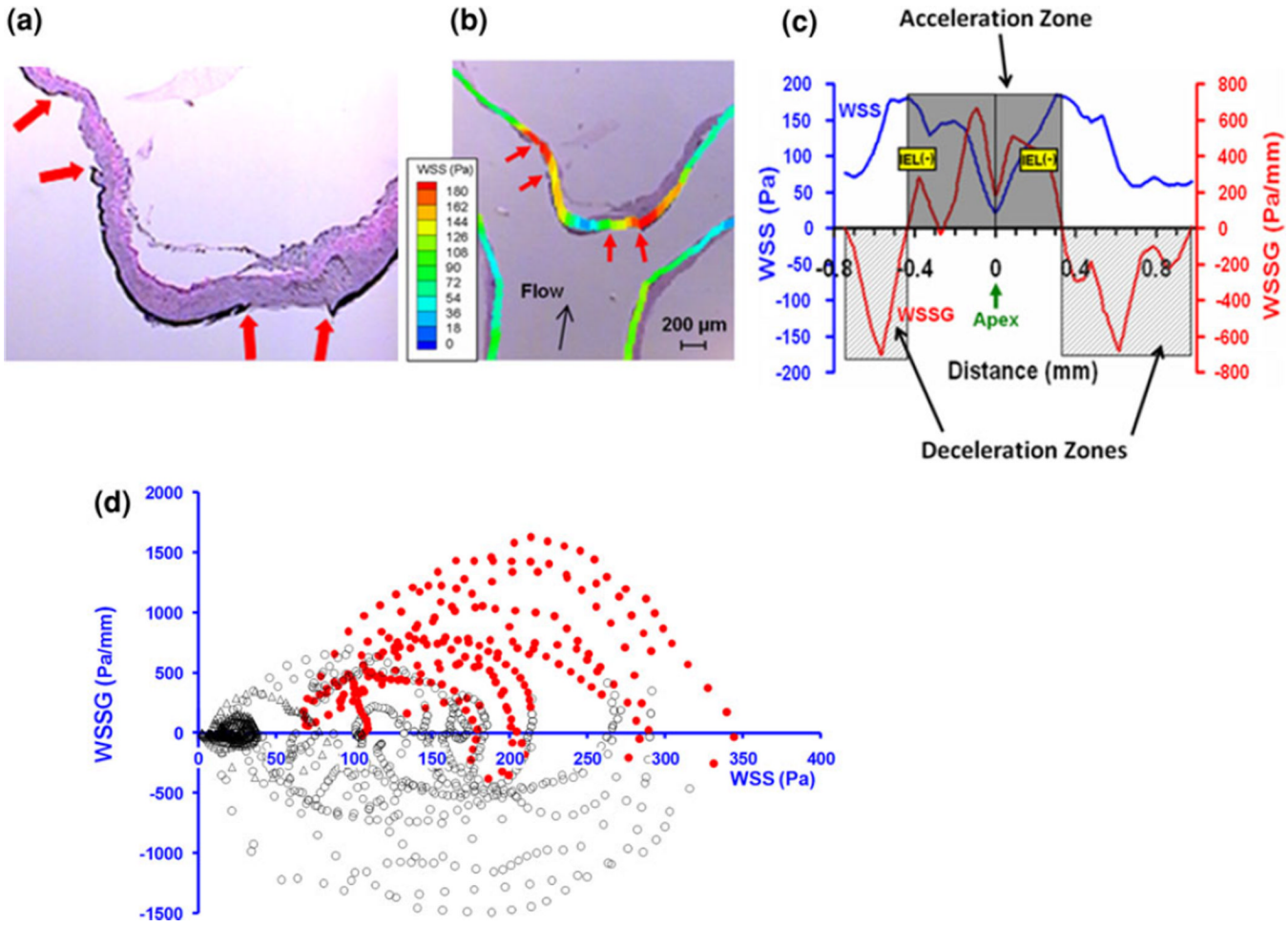

FIGURE 3.

Hemodynamic conditions for aneurysm initiation at the basilar terminus in rabbits that received bilateral CCA ligation.[79] (a) Histology (Van Gieson staining) at 5 days showing early aneurysmal damage in the form of IEL loss in two segments (ends are marked by arrows) flanking the apex. (b) Hemodynamics-histology co-mapping to determine the local hemodynamic conditions of initial aneurysmal damage. (c) WSS (blue) and WSSG (red) distribution along the wall, whereby IEL damage (yellow bands) localized in the flow acceleration zone. (d) "Point cloud" showing microsegments of intact IEL (black open circles) and damaged IEL (red solid dots) plotted against their local WSS and WSSG values. The red dots are clustered to the top right of the coordinate system, indicating that aneurysm-initiating conditions are positive WSSG and high WSS. Reproduced from Metaxa *et al.*[79] with permission.

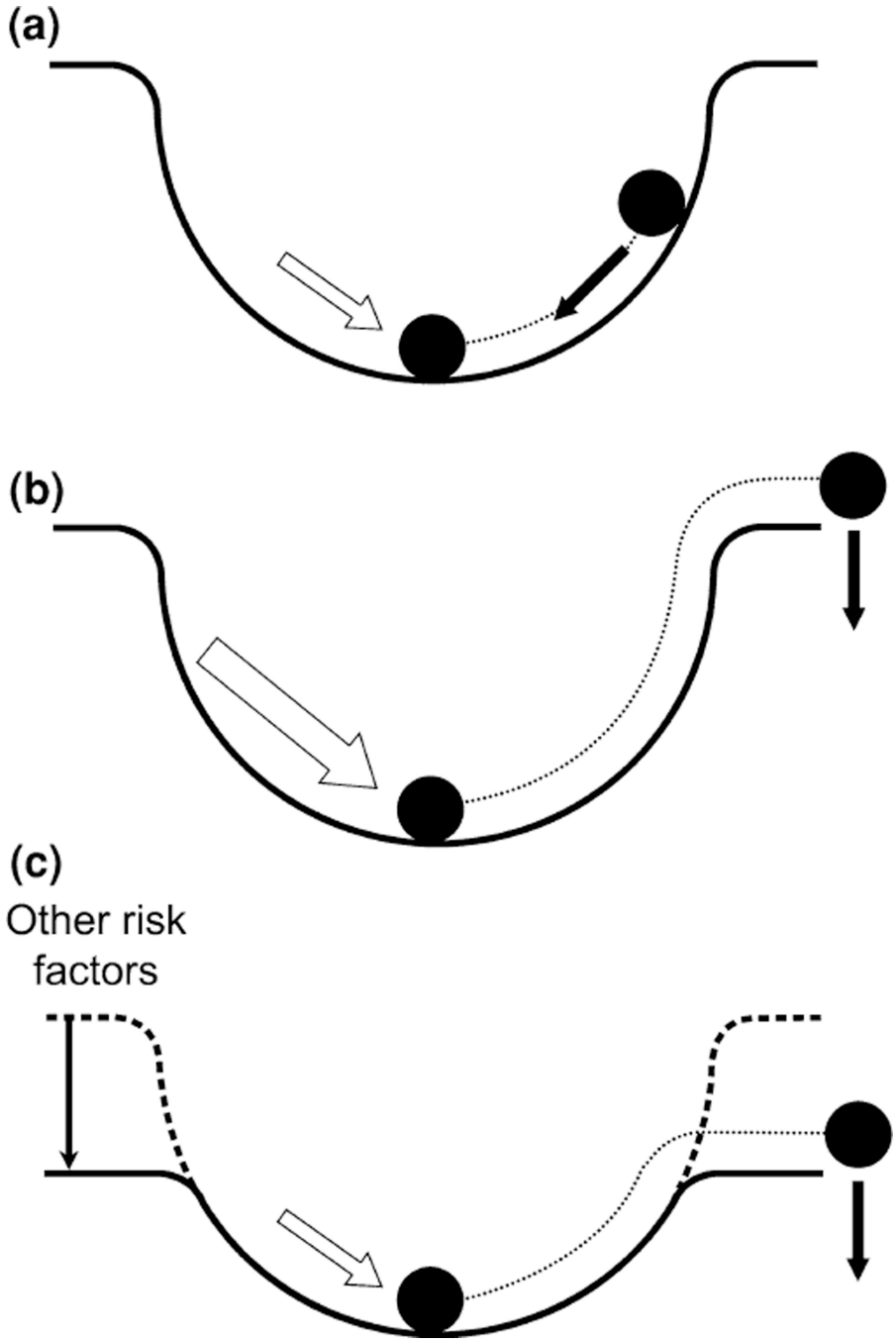

FIGURE 4.

A marble-in-a-bowl metaphor for the role of hemodynamic insult in relation to other risk factors in aneurysm initiation. Homeostasis is represented by the marble at the bottom of the bowl and hemodynamic insult (white arrow) is represented by a push on the marble. (a) A gentle push results in a return to homeostasis. (b) A strong enough push causes the marble to fall out of the bowl causing a departure from homeostasis into pathogenesis. (c) Other risk factors (family history, female gender, genetic diseases, cigarette smoking and hypertension) lower the rim of the bowl, such that a gentle push can result in pathogenesis (i.e., aneurysm formation). Modified from Meng *et al.*[77]

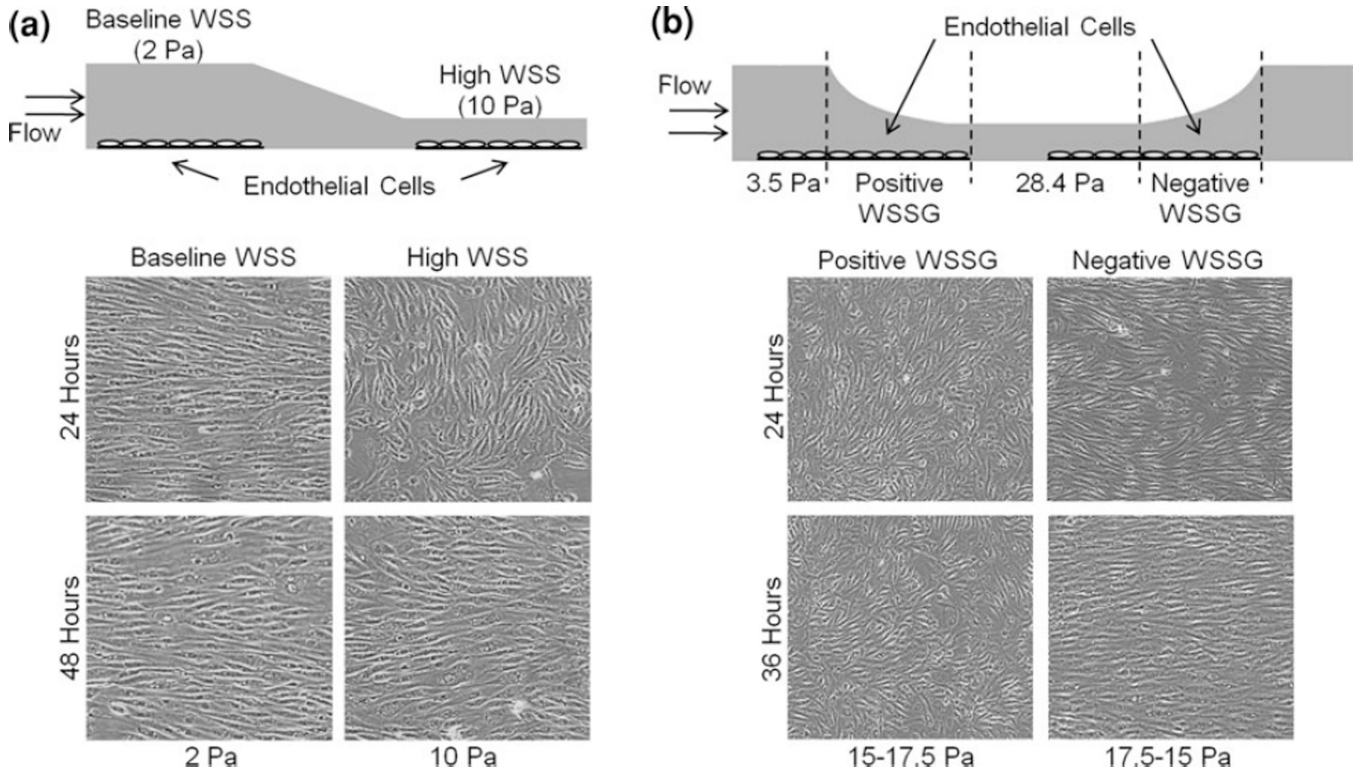

FIGURE 5.

Alignment of bovine aortic ECs subjected to high WSS alone (a) or in combination with WSSG (b). (a) *In vitro* flow chamber subjecting EC monolayers to baseline WSS and high WSS.[18] ECs align and elongate with their long axis parallel to the flow with a time course dependent on the WSS and display a transient perpendicular alignment when WSS is high. (b) *In vitro* flow system with converging and diverging-segments to produce positive and negative WSSG across EC monolayers.[17] Positive WSSG hinders cell alignment to flow while negative WSS promotes it, even under the same range of WSS. Modified from Dolan et al.[20,21] Reproduced with permission.

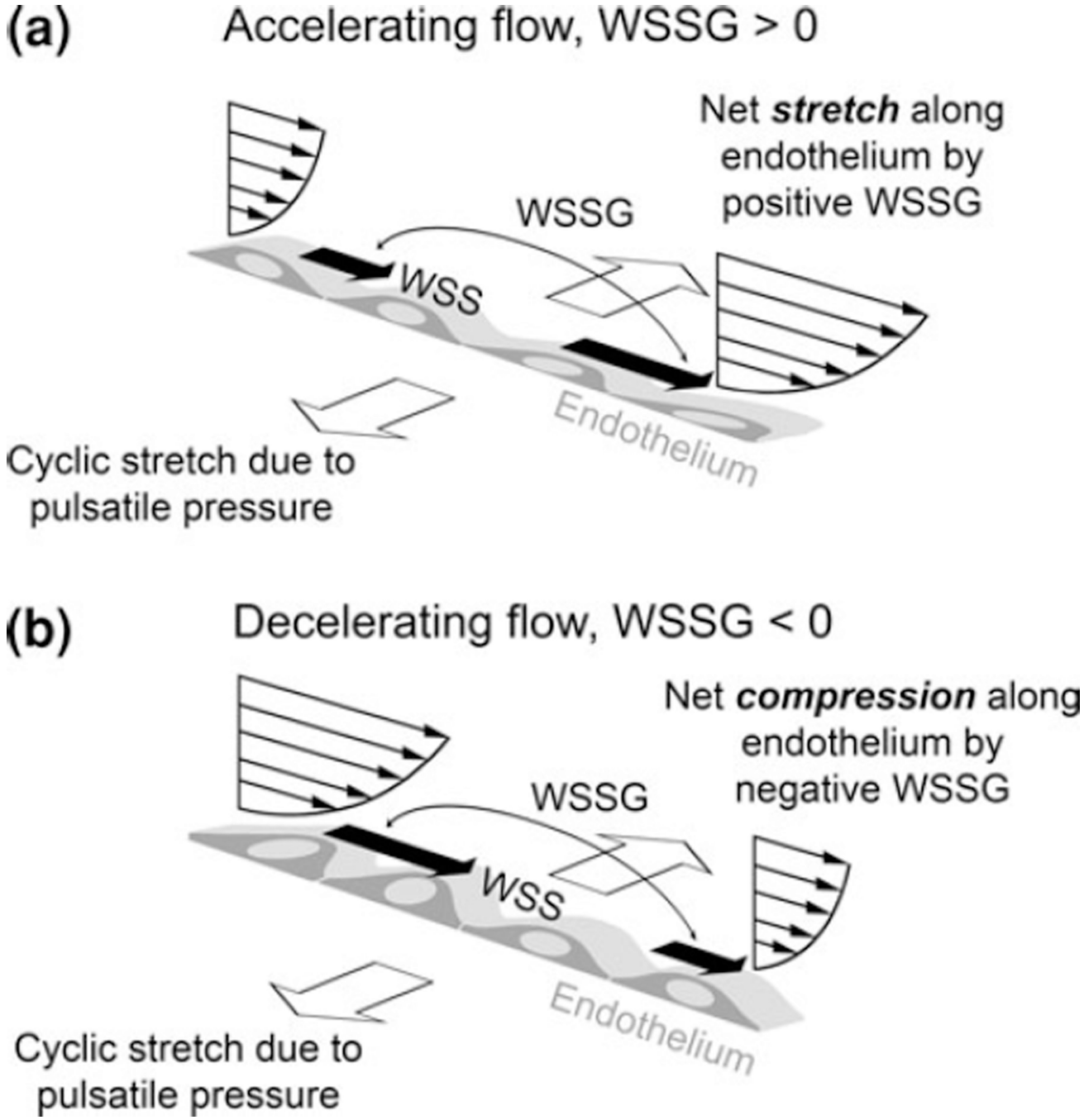

FIGURE 6.
A conceptual picture of the mechanical forces on ECs in accelerating and decelerating flow: WSS from the flowing blood, net stretching/compression due to WSSG, and cyclic stretching from pulsatile pressure.